NAVAL POSTGRADUATE SCHOOL
Monterey, California

THESIS

D17233

REAL TIME ADAPTIVE CONTROL OF AN
AUTONOMOUS UNDERWATER VEHICLE (AUV)

by

Michael H. Davis

September 1989

Thesis Advisor: Roberto Cristi

Approved for public release; distribution is unlimited

REPORT DOCUMENTATION PAGE

Form Approved
OMB No. 0704-0188

1a REPORT SECURITY CLASSIFICATION UNCLASSIFIED	1b RESTRICTIVE MARKINGS
2a SECURITY CLASSIFICATION AUTHORITY	3 DISTRIBUTION/AVAILABILITY OF REPORT Approved for public release; distribution is unlimited
2b DECLASSIFICATION/DOWNGRADING SCHEDULE	
4 PERFORMING ORGANIZATION REPORT NUMBER(S)	5 MONITORING ORGANIZATION REPORT NUMBER(S)
6a NAME OF PERFORMING ORGANIZATION Naval Postgraduate School 6b OFFICE SYMBOL (If applicable) 62	7a NAME OF MONITORING ORGANIZATION Naval Postgraduate School
6c ADDRESS (City, State, and ZIP Code) Monterey, California 93943-5000	7b ADDRESS (City, State, and ZIP Code) Monterey, California 93943-5000
8a NAME OF FUNDING/SPONSORING ORGANIZATION 8b OFFICE SYMBOL (If applicable)	9 PROCUREMENT INSTRUMENT IDENTIFICATION NUMBER
8c ADDRESS (City, State, and ZIP Code)	10 SOURCE OF FUNDING NUMBERS PROGRAM ELEMENT NO / PROJECT NO / TASK NO / WORK UNIT ACCESSION NO

11 TITLE (Include Security Classification)
REAL TIME ADAPTIVE CONTROL OF AN AUTONOMOUS UNDERWATER VEHICLE (AUV)

12 PERSONAL AUTHOR(S)
DAVIS, Michael H.

13a TYPE OF REPORT	13b TIME COVERED	14 DATE OF REPORT (Year, Month, Day)	15 PAGE COUNT
Engineer's Thesis	FROM _____ TO _____	September 1989	68

16 SUPPLEMENTARY NOTATION The views expressed in this thesis are those of the author and do not reflect the official policy of the Department of Defense or the U.S. Government.

17 COSATI CODES		
FIELD	GROUP	SUB-GROUP

18 SUBJECT TERMS (Continue on reverse if necessary and identify by block number)
Autonomous Underwater Vehicle; Variable Structure Control; AUV; Sliding Mode Control; Doyle-Stein Observer; Adaptive Control

19 ABSTRACT (Continue on reverse if necessary and identify by block number)

In this research the problem of designing a controller for the dive maneuver of an Autonomous Underwater Vehicle (AUV) is addressed. The highly nonlinear nature of the vehicle dynamics and the requirement for the fast maneuvering call for robust control techniques. In particular Variable Structure Control (VSC) combined with Adaptive Control (AC) techniques seem to yield satisfactory performance in terms of robustness, capability to adjust to different operating conditions, and speed of response. Also linear robust techniques based on LQG and robust observers are presented to address the case when the whole state (in terms of pitch rate, pitch, and depth) is not available for measurement.

20 DISTRIBUTION/AVAILABILITY OF ABSTRACT	21 ABSTRACT SECURITY CLASSIFICATION
☒ UNCLASSIFIED/UNLIMITED ☐ SAME AS RPT ☐ DTIC USERS	UNCLASSIFIED
22a NAME OF RESPONSIBLE INDIVIDUAL Roberto Cristi	22b TELEPHONE (Include Area Code) 408-646-2223 / 22c OFFICE SYMBOL 62Cx

DD Form 1473, JUN 86 Previous editions are obsolete SECURITY CLASSIFICATION OF THIS PAGE

S/N 0102-LF-014-6603

UNCLASSIFIED

T245414
T24522

Approved for public release; distribution is unlimited

Real Time Adaptive Control of an Autonomous Underwater Vehicle (AUV)

by

Michael H. Davis
Lieutenant, United States Navy
B.S.E.E., San Diego State University, 1983

Submitted in partial fulfillment
of the requirements for the degree of

MASTER of SCIENCE in ELECTRICAL ENGINEERING
and
ELECTRICAL ENGINEER

from the

NAVAL POSTGRADUATE SCHOOL
September 1989

ABSTRACT

In this research the problem of designing a controller for the dive maneuver of an Autonomous Underwater Vehicle (AUV) is addressed. The highly nonlinear nature of the vehicle dynamics and the requirement for fast maneuvering call for robust control techniques. In particular, Variable Structure Control (VSC) combined with Adaptive Control (AC) techniques seem to yield satisfactory performance in terms of robustness, capability to adjust to different operating conditions, and speed of response. Also, linear robust techniques based on LQG and robust observers are presented to address the case when the whole state (in terms of pitch rate, pitch and depth) is not available for measurement.

DU7233
C.1

TABLE OF CONTENTS

I. INTRODUCTION..... 1

II. MODELING OF THE AUV..... 5

A. BASIC DEFINITIONS..... 5

B. LINEAR MODEL..... 7

C. STABILITY METHODOLOGY..... 10

III. VARIABLE STRUCTURE CONTROL..... 12

A. INTRODUCTION.....12

B. VSC THEORY.....13

C. APPLICATION OF VSC TO TRACKING.....16

D. VSC EXAMPLE.....18

E. VSC WITH ADAPTIVE COMPENSATION.....23

F. SIMULATIONS AND RESULTS.....26

IV. LINEAR ROBUST CONTROL OF THE AUV.....30

A. INTRODUCTION.....30

B. ROBUST OBSERVERS AND THE DOYLE-STEIN CONDITION....31

C. SIMULATIIONS AND RESULTS.....36

V. AUV ARCHITECTURE.....41

A. INTRODUCTION.....41

B. HARDWARE ALTERNATIVES.....42

C. OPERATING EXAMPLES.....48

D. OBSERVATIONS.....53

VI. CONCLUSIONS.....56
A. RESULTS.....56
B. FUTURE RESEARCH.....56
LIST OF REFERENCES.....58
INITIAL DISTRIBUTION LIST.....60

ACKNOWLEDGEMENTS

I would like to express my sincerest thanks to Professor Roberto Cristi for his immense help and encouragement with this thesis. Most of this thesis and the algorithms within it are based upon his ideas in Variable Structure Control (VSC). In general all the people associated with the AUV project (Professor A. Healy: principal investigator) stimulated my interests in underwater vehicles and in particular the VSC method of control. I would also like to thank my classmates for their support and assistance with a special acknowledgement to Stephen Spehn who helped me through many a rough spot. Finally, I would like to thank my wife Beth for her support and understanding during these last two and a half years (most of it spent apart from one another). A truer friend would be hard to find.

I. INTRODUCTION

In the last few years, considerable interest in Autonomous Underwater Vehicles (AUV) has arisen. Possible utilization scenarios for an untethered submersible have also grown and include: sea floor mapping, target identification, remote reconnaissance, object recovery, etc. A typical mission would include downloading of the mission program, remote positioning and launch, subsequent vehicle recovery, and data collection. AUV vehicles now in design or production can employ basically any shape from a box shape suited to offshore work to a body of revolution suited for high speed maneuverability or long distance missions. The AUV group at the Naval Postgraduate School (NPS) has chosen the shape shown in Figure 1 which was derived from the Swimmer Delivery Vehicle (SDV) [Ref. 1]. Part of the rationale was that, since extensive data exists on that particular design, it would facilitate calculation of a reasonably accurate analytical model for a similar but smaller scale model. This is particularly advantageous to the design of a control system for the AUV, since knowledge of an accurate dynamic model is in general the basis of a reliable control design. Also, tests conducted by computer

simulations yield results which are closer to the physical performance of the vehicle.

The initial goal of the AUV group is to build a working prototype AUV that will be able to expand its capabilities to meet the increased complexity of future missions.

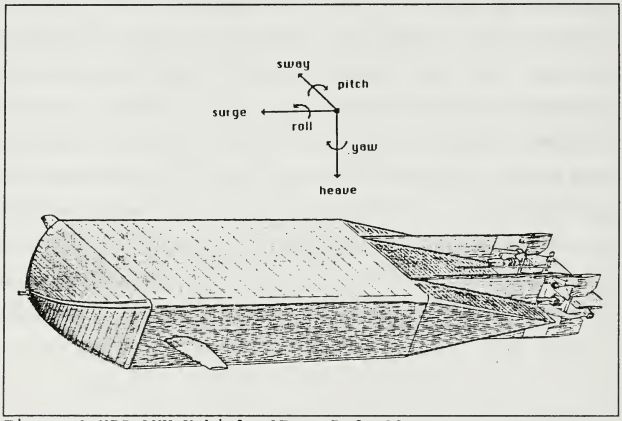

Figure 1 NPS AUV Vehicle [From Ref. 2]

As with all analytical models of submersibles, the equations of motion are highly nonlinear and vary with speed and the amount of equipment onboard. Adding to that is the difficulty in obtaining exact dynamic coefficients. Because of the high level of nonlinearities and model uncertainties, we have to consider more sophisticated design techniques. Recently, an adaptive controller has been designed by Schwartz

[Ref. 2] where the parameters of a compensator are adjusted on-line on the basis of an estimated transfer function. This approach has not only provided insight for the overall control design, but it has also provided parameters of the linearized dynamics.

The adaptive controller by Schwartz has proved to yield satisfactory behavior in terms of speed of response and robustness in the presence of model changes. On the other hand, the computational complexity involved in the adaptive controller calls for investigation of simpler techniques which do not require complex manipulation of matrices to be performed in real time.

With these motivations in mind (mainly adaptability and robustness in the presence of uncertainties), we have investigated an alternative control technique based on Variable Structure Control (VSC). It will be shown that a simple and robust nonlinear controller can be designed, combined with an adaptive loop which compensates for some of the model uncertainties.

The exciting part of the VSC approach is that the design can be based on a nominal model (usually available from test runs and/or physical insight) and a bound on the uncertainty of the model. This gives to the designer the possibility of using this simple nominal model, possibly linear, while still preserving the global stability of the controlled system.

Situations which exhibit coupled dynamics can be handled by VSC design techniques, and simple and robust controllers can be designed by including the effects of coupling in the model uncertainty.

A further aspect of this research is the investigation of the performance of a robust linear controller in the presence of uncertainties and nonlinearities. In particular we address the problem of control when the full state is not available for measurement. This is the case, for example, when in a diving maneuver we measure depth alone, rather then depth, pitch and pitch rate. It turns out that the design of a "robust" observer (in a sense which will be clarified in a later section) together with an optimal controller can still be satisfactory, under limited ranges of the operating conditions.

An outline of the thesis is as follows. Chapter II covers modeling of the AUV and stability analysis, while Chapter III addresses the controller design by Variable Structure Control. In Chapter IV a controller design based on the theory of Robust Observers is presented with applications to the AUV. Alternative hardware realizations are surveyed in Chapter V, while conclusions and recommendations for future research are the subjects of the concluding chapter.

II. MODELING OF THE AUV

A. BASIC DEFINITIONS

The dynamics of underwater vehicles are nonlinear and are affected by uncertainties due to modeling errors (data sampling, sensors, electrical noise, physical measurements, hydrodynamic coefficients, etc.) and external disturbances (currents, tether, surfaces, etc.). In general, a linear controller for a vehicle which moves in "n" degrees of freedom should be linearized about its respective axes at sufficiently different speeds and then some form of "gain scheduling" is usually implemented. A mathematical model of the AUV can be obtained by accounting for the hydrodynamic forces acting upon it. In particular, the model results in a set of highly nonlinear differential equations in state space form

$$\dot{\underline{x}} = f(\underline{x},u,t) \qquad (2.1a)$$

where $\underline{x}$ is the vector of position and velocities (both absolute and angular) of the vehicle. The state vector $\underline{x}$ is comprised of

x ≡ surge	ϕ ≡ roll
y ≡ sway	θ ≡ pitch
z ≡ heave	ψ ≡ yaw

which represent position (absolute and angular) in a global coordinate frame, and

u ≡ surge rate p ≡ roll rate

v ≡ sway rate q ≡ pitch rate

w ≡ heave rate r ≡ yaw rate

which represent velocities in a body fixed coordinate frame. Therefore the full state vector $\underline{x}$ in the differential equation becomes $\underline{x}=[u,v,w,p,q,r,x,y,z,\phi,\theta,\psi]'$.

In a diving maneuver the only states of interest for this diving controller are depth (z), pitch (Θ) and pitch rate (q) while the input we consider is the dive fin (stern plane) deflection angle (d). Therefore the dynamic equations become

$$\dot{\underline{x}}=f(\underline{x},d) \qquad (2.1b)$$

where

$$\underline{x}=[q,\theta,z] \qquad (2.1c)$$

and d is the stern plane dive command. Simulations conducted using the full nonlinear model [Ref. 2] show that, within the neighborhood of operating conditions (i.e., cruising at a constant speed), a linear model yields a fairly reasonable fit. This has also been confirmed by data collected from the prototype [Ref. 1].

The basic structure of the dynamic model considered is shown in Figure 2. The nonlinear model accounts for perturbations around the linear model which are caused by various hydrodynamic effects (currents, cavitation, surface effects, etc.). These effects have the tendency to perturb the AUV from the nominal trajectory, thus acting like an extra

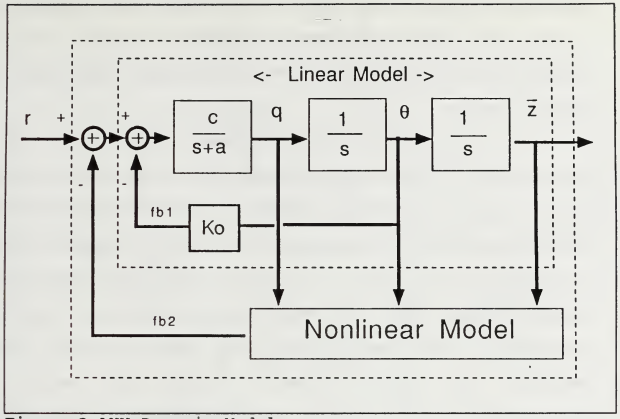

Figure 2 AUV Dynamic Model

component on the stern plane. Therefore, we can model this effect by the feedback signal $fb_2(t)$ (shown in Figure 2) which adds a perturbation to the dive plane as

$$fb_2(t) = f(q(t),\Theta(t),z(t),t). \qquad (2.2)$$

We can assume that the perturbation is time-varying and depends on pitch rate, pitch, and heave (depth).

B. LINEAR MODEL

To develop a specific linear model which approximates the dynamics, let us consider a structure of the form shown in Figure 3(a). For simplicity, let G(s) be a first order transfer function and also note that this model does not

contain a feedback from $\Theta(t)$ to the input (i.e., the gain K_o in Figure 2). There are several reasons to believe that this feedback gain is required. First, physically, the equalizing moments are

$$J\ddot{q} = F_1(d(t)) + F_2(\Theta(t)) + F_3 \qquad (2.3)$$

where $F_1(d(t))$ is the torque around the center of gravity due to the stern plane angle, $F_2(\Theta(t))$ is the torque due to the displacement between the Center of Gravity (CG) and the Center of Buoyancy (CB), and F_3 is the balance of the hydrodynamic moments acting over the body of the vehicle (including hydrodynamic added inertia, drag, and angle of attack induced moments). For small values of $\Theta(t)$, this effect is proportional to $\Theta(t)$ itself, as diagrammed in Figure 3(b). Second, it has been shown in Reference 2 that the response of the dynamics relating $d(t)$ and $\Theta(t)$ from an imparted impulse to the stern plane yields a pitch $\Theta(t)$ which decays to zero. This indicates that all the poles of the transfer function between $d(t)$ and $\Theta(t)$ are stable. Finally, as speed increases, we expect that the stabilizing effect due to the feedback gain K_o decreases because other hydrodynamic forces become more dominant. The result is that the dominant poles of the transfer function from $d(t)$ to $\Theta(t)$ follow a root locus path as shown in Figure 3(c). [Ref. 2]

Following this formulation, the linearized state-space mathematical model for the AUV in a dive maneuver is

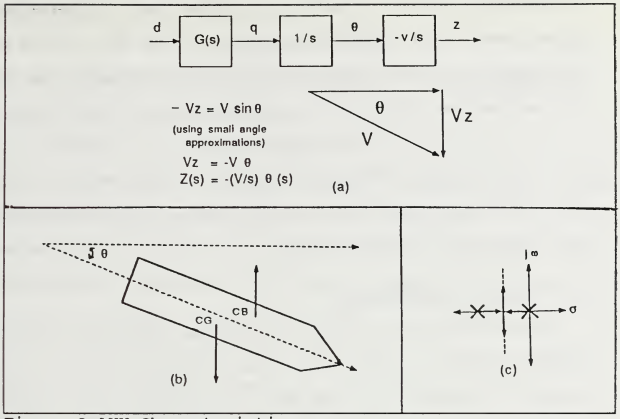

Figure 3 AUV Characteristics

$$\dot{\underline{x}} = \begin{vmatrix} -a & -K_0 & 0 \\ 1 & 0 & 0 \\ 0 & 1 & 0 \end{vmatrix} \underline{x} + c \begin{vmatrix} 1 \\ 0 \\ 0 \end{vmatrix} (d(t) - f(\underline{x})) \qquad (2.4a)$$

$$z = [\ 0\ 0\ -v\ ]\ \underline{x} \qquad (2.4b)$$

$$\underline{x} = [\ q\ \theta\ \overline{z}\ ]' \qquad (2.4c)$$

where we define the "normalized depth" as

$$\overline{z} = (-1/v)z \qquad (2.4d)$$

with v being the forward velocity of the AUV. The fact that the system is in controllable canonical form will be instrumental in the design of the control system. The parameters a, c and K_0 in (2.4a) depend on the operating

conditions (speed, primarily) of the vehicle, and can be determined on the basis of test runs of the AUV. On the basis of these runs we can determine nominal values a_o, c_o and K_o for the parameters and write the dynamics as

$$\dot{x} = A_o x + b(d + f) \tag{2.5}$$

and design the controller based on this model. In the following chapters control system design techniques based on this model will be presented.

C. STABILITY METHODOLOGY

Most methods of stability criteria, including Routh and Nyquist, are not applicable to nonlinear systems. The second method of Lyapunov is the most general test for stability analysis. According to this approach we define stability (in the sense of Lyapunov) and a criterion for stability as follows.

Definition: Given a nonlinear system

$$\dot{x} = f(x,u,t) \tag{2.6}$$

and an equilibrium point x_e, such that $f(x_e,u,t) = 0$, we say that x_e is a stable equilibrium point (in the sense of Lyapunov) provided that for all $\epsilon > 0$ there exists a $\delta_\epsilon > 0$ (where δ depends on ϵ) such that all trajectories of (2.6) for which $\|\underline{x}(0)-x_e\| < \epsilon$ do not leave a ball of radius δ_ϵ around x_e, i.e., $\|\underline{x}(t)-x_e\| < \delta_\epsilon$ for all $t \geq 0$.

Definition: If x_e is stable and

$$\lim_{t\to\infty} \underline{x}(t) = x_e \tag{2.7}$$

for any initial condition $\underline{x}(0)$, then x_e is an asymptotically stable equilibrium point. [Ref. 3]

A method to determine whether an equilibrium point is stable or not is by the second method of Lyapunov. This method is quite convenient for the stability analysis of nonlinear systems since it does not require explicit solutions of the differential equations. To briefly summarize the method, consider a system described by the differential equation $\dot{x}=f(x,t)$ with $f(0,t)=0$ for all time. If there exists a differentiable scalar function $V(x,t)$ such that $V(x,t)$ is positive definite and $\dot{V}(x,t)$ is negative definite, then the equilibrium point is asymptotically stable. A precise statement of the method is presented in Reference 3.

Given this definition of stability and the AUV model presented earlier, we were ready to design a controller. A nonlinear design method using Variable Structure Control (VSC) was then followed.

III. VARIABLE STRUCTURE CONTROL

A. INTRODUCTION

The nonlinear dynamics of the AUV can be described by

$$\dot{\underline{x}} = f(\underline{x},u,t) \tag{3.1}$$

and present a high degree of uncertainty due to several factors. In spite of the highly nonlinear behavior we can still approximate the dynamics of the AUV by a linear component and a nonlinear perturbation

$$\dot{\underline{x}} = A\underline{x} + \underline{b}(d + f(\underline{x})). \tag{3.2}$$

In the particular case of a diving maneuver, the state of equation (3.2) is given by $\underline{x} = [q,\theta,\bar{z}]'$ and the dynamics (3.2) assume a controllable canonical form structure (see (2.4a)).

The aim of the controller in a diving maneuver (like in many similar problems) is to drive the state vector $\underline{x}$ to track a desired state $\underline{x}_d$. In other words, given a desired state $\underline{x}_d \in \mathfrak{R}^n$ of the form

$$\underline{x}_d(t) = [x_d^0(t),\cdots,x_d^{(n-1)}(t)]' \tag{3.3}$$

we want to design a controller such that the error signal

$$\underline{e}(t) = \underline{x}(t) - \underline{x}_d(t) \tag{3.4}$$

tends to zero as $t \to \infty$. Furthermore we want all signals in the loop to be bounded for all time.

In our particular case the desired signal $\underline{x}_d$ is represented by the desired depth, pitch and pitch rate. Since

in steady state (i.e., cruising at a constant depth) pitch and pitch rate are zero, we define $\underline{x}_d$ as

$$\underline{x}_d = [0\ 0\ -z_d/v]' \tag{3.5}$$

with z_d being desired depth.

Due to the presence of the uncertainty f(x) in (3.2), a control solution which guarantees a sufficient stabilty margin has to be devised. The Variable Structure Control (VSC) (also called the Sliding Mode (SM)) technique is at the basis of the controller we propose for the AUV.

B. VSC THEORY

The idea behind using the VSC method on a dynamic system

$$\dot{\underline{x}} = f(\underline{x},u,t) \tag{3.6}$$

with $\underline{x} \in \mathfrak{R}^n$ and $u \in \mathfrak{R}^1$ is to drive the state from any initial condition $\underline{x}(0)$ onto a sliding surface

$$s(\underline{x}) = 0 \tag{3.7}$$

of the state space in a finite time and to keep the state on the surface for all subsequent times. Although the surface (3.7) can be chosen in a fairly arbitrary fashion, it nevertheless must be associated with stable dynamics. In particular, the surface $s(\underline{x}(t)) = 0$ for all $t \geq t_o$ must imply

$$\lim_{t\to\infty} \underline{x}(t) = 0 \tag{3.8}$$

In most applications the sliding surface is a linear function of the state, in the sense that (3.7) is chosen as

$$s(\underline{x}) = \underline{c}'\underline{x} \tag{3.9}$$

for some vector $\underline{c}' \in \mathfrak{R}^n$.

From the statements presented in the last paragraph, the terminology of Sliding Mode is evident, since the state, once taken from the initial condition $\underline{x}(0)$ onto the surface $s(\underline{x}) = 0$, "slides" to zero on this surface by virtue of (3.8) (see Figure 4). Apart from the requirement of being associated with stable dynamics, a surface in $\mathfrak{R}^n$ is a sliding surface provided

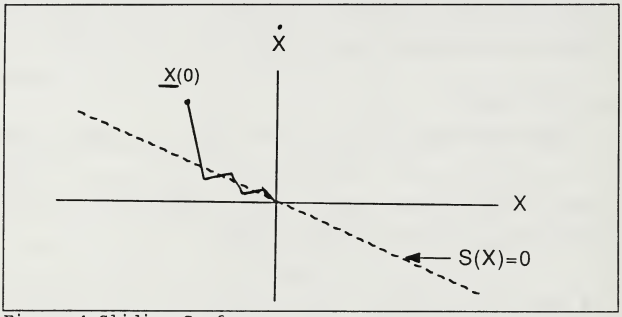

Figure 4 Sliding Surface

that we can determine a control input signal such that

$$s(\underline{x}(t))\dot{s}(\underline{x}(t)) < 0 \qquad (3.10)$$

whenever $s(\underline{x}(t)) \neq 0$. The reason behind condition (3.10) is that the definition of the Lyapunov function

$$V(\underline{x}) = 0.5s^2(\underline{x}) \qquad (3.11)$$

yields

$$\dot{V}(\underline{x}) = s(\underline{x})\dot{s}(\underline{x}) \qquad (3.12)$$

along the trajectories of (3.6), and therefore the condition $\dot{V}(\underline{x}) < 0$ (given by (3.10)) makes $s^2(\underline{x})$ a monotonically decreasing function so that $s\{\underline{x}(t)\}$ tends to zero. Moreover, if we "strengthen" condition (3.10) by imposing

$$s\{\underline{x}(t)\}\dot{s}\{\underline{x}(t)\} \leq -\eta|s\{\underline{x}(t)\}| \tag{3.13}$$

with η a positive constant, then it is easy to see that the sliding surface $s(\underline{x}) = 0$ is reached in a finite time. This can be seen by writing (3.13) as

$$\dot{s}\{\underline{x}(t)\} \leq -\eta\,\mathrm{sgn}\{s(\underline{x}(t)\} \tag{3.14}$$

where we define the sgn function as

$$\mathrm{sgn}(s) = \begin{cases} +1 & \text{if } s > 0 \\ -1 & \text{if } s < 0 \\ 0 & \text{if } s = 0 \end{cases} \tag{3.15}$$

On the basis of these conditions, if we restrict ourselves to linear sliding surfaces ($s(\underline{x}) = \underline{c}'\underline{x}$ as in (3.9)), then we obtain from (3.14) and (3.6)

$$\dot{s}\{\underline{x}(t)\} = \underline{c}'f(\underline{x},\underline{u},t) \leq -\eta\,\mathrm{sgn}\{s(\underline{x})\} \tag{3.16}$$

for which the control u(t) must be such that

$$u(t) = \begin{cases} u_+(t) & \text{if } \mathrm{sgn}\{s(x)\} > 0 \\ u_-(t) & \text{if } \mathrm{sgn}\{s(x)\} < 0 \end{cases} \tag{3.17}$$

and u_+ and u_- are such that

$$\underline{c}'f(x,u_+,t) \leq -\eta \tag{3.18a}$$

$$\underline{c}'f(x,u_-,t) \geq \eta \tag{3.18b}$$

with η being a positive constant parameter of the controller. As a matter of fact, η does not have to be a constant and, in general, it can be made a function of the state $\eta(\underline{x})$. From the

definition of the control action (3.17) the terminology of Variable Structure Control (VSC) becomes evident, since the control assumes different structures (u_+ and u_-) according to which side of the sliding surface the state is on (i.e., according to the sign of $s(\underline{x})$).

C. APPLICATION OF VSC TO TRACKING

A particularly interesting situation arises when the dynamic model (3.6) can be written in the form

$$\dot{\underline{x}} = f(\underline{x}) + b(\underline{x})u(t) \tag{3.19}$$

where nominal values of $\hat{f}$ and $\hat{b}$ corresponding to f and b in (3.19) are known. For simplicity assume that b(x) is completely known (this will be relaxed at the end of the section). We can write f(x) as

$$\underline{f}(\underline{x}) = \hat{\underline{f}}(\underline{x}) + \Delta\underline{f}(\underline{x}) \tag{3.20}$$

with Δf representing the uncertainty in $f(\underline{x})$, and we assume to know some bound on $|\Delta f(\underline{x})|$ to be specified later. Given a desired state $\underline{x}_d(t)$, we want to apply the sliding mode technique in order to move the state $\underline{x}(t)$ of the system to track the desired trajectory $\underline{x}_d(t)$. In order to do this we define the error as

$$\underline{e}(t) = \underline{x}(t) - \underline{x}_d(t) \tag{3.21}$$

and a generic surface as

$$s(\underline{e}) = \underline{c}'\underline{e} \tag{3.22}$$

for some vector $\underline{c}' \in \mathfrak{R}^n$. Combining (3.19), (3.20), (3.21) and (3.22) we obtain

$$\underline{c}'(\dot{\underline{x}} - \dot{\underline{x}}_d) = \underline{c}'\hat{\underline{f}}(\underline{x}) + \underline{c}'\Delta\underline{f}(\underline{x}) - \underline{c}'\dot{\underline{x}}_d(t) + \underline{c}'\underline{b}(\underline{x})u(t). \quad (3.23)$$

An important feature of (3.23) is that the right hand side is the sum of terms which are known at all times $\{\underline{c}'\hat{f}(\underline{x}) - \underline{c}'\dot{\underline{x}}_d(t)\}$, an uncertain term $\{\underline{c}'\Delta\underline{f}(\underline{x})\}$ and the control term $\{\underline{c}'\underline{b}(\underline{x})u(t)\}$. For this reason we can separate the control input u(t) into two terms as

$$u(t) = \hat{u}(t) + \bar{u}(t) \quad (3.24)$$

with $\hat{u}(t)$ compensating for the "nominal" dynamics, i.e.,

$$\underline{c}'\hat{\underline{f}}(\underline{x}) - \underline{c}'\dot{\underline{x}}_d(t) + \underline{c}'\underline{b}(\underline{x})\hat{u}(t) = 0 \quad (3.25)$$

and $\bar{u}(t)$ compensating for the uncertainty Δf. Combining (3.23), (3.24) and (3.25), we obtain

$$\underline{c}'\dot{\underline{e}} = \underline{c}'\Delta\underline{f} + \underline{c}'\underline{b}\bar{u} \quad (3.26)$$

and we can determine the input component $\bar{u}$ in order to drive the state $\underline{e}(t)$ on to the sliding surface as

$$s\{\underline{e}(t)\} = \underline{c}'\underline{e}(t) = 0. \quad (3.27)$$

This determination can be accomplished by choosing $\bar{u}(t)$ so as to satisfy (3.18), which leads to the control

$$\bar{u}(t) = -F(\underline{x},t)\,\mathrm{sgn}\{\underline{c}'\underline{e}(t)\} \quad (3.28)$$

with $F(\underline{x},t)$ a known function of the state, such that

$$F(\underline{x},t) > |\underline{c}'\Delta f(x)|/|\underline{c}'\underline{b}(x)|. \quad (3.29)$$

Clearly a condition which has to be satisfied is that $\underline{c}'\underline{b}(\underline{x}) \neq 0$ for all time.

In conclusion, if $\underline{c}'$ is such that $\underline{c}'\underline{e}(t) = 0$ (which implies $\underline{e}(t) \rightarrow 0$), then we can say that the control input from (3.28), (3.29) and (3.25)

$$u(t) = \hat{u}(t) + \bar{u}(t) = -(1/\underline{c}'\underline{b})\{\underline{c}'\hat{\underline{f}}(\underline{x}) - \underline{c}'\dot{\underline{x}}_d(t)\} + F(\underline{x},t)\,\mathrm{sgn}(\underline{c}'\underline{e}(t)) \qquad (3.30)$$

yields the following:

- the error $\underline{e}(t)$ is driven to the sliding surface $\underline{c}'\underline{e} = 0$ in a finite time, and
- $e(t) \rightarrow 0$ as $t \rightarrow \infty$.

A very important point is that, once the state is on the sliding surface, the decay of $\underline{e}(t)$ is determined by the vector $\underline{c}'$ only. [Ref. 4]

D. VSC EXAMPLE

To illustrate the sliding mode design process, let us implement it on a second order system described by

$$x^{(2)} = f(\underline{x},t) + b(\underline{x})u(t) + p(t) \qquad (3.31)$$

where we define the state $\underline{x}(t) = [x^{(1)}\ x]'$, the desired state $\underline{x}_d = [x_d^{(1)}\ x_d]'$ and the vector $\underline{c}' = [1\ \lambda]$ (with $\lambda > 0$). While $f(\underline{x},t)$ is not known precisely, we assume that nominal values $\hat{f}(\underline{x},t)$ are known, for which

$$f(\underline{x},t) = \hat{f}(\underline{x},t) + \Delta f(\underline{x},t) \qquad (3.32)$$

with $\Delta f(\underline{x},t)$ having a known upper bound of

$$F(\underline{x},t) \geq |\Delta f(\underline{x},t)|. \qquad (3.33)$$

The estimate $\hat{f}(\underline{x},t)$ is available from several sources where, for example, a nominal model could be generated from

experimental data and parameter estimation techniques. If the control gain $b(\underline{x},t)$ is also uncertain, then we assume that it is bounded by a function $B(\underline{x},t)$ where the gain is known within a certain ratio

$$1/B(\underline{x},t) \leq \hat{b}(\underline{x},t)/b(\underline{x},t) \leq B(\underline{x},t). \qquad (3.34)$$

Also, the perturbations $p(t)$ are assumed to be unknown and bounded by a continuous time function

$$P(t) \geq |p(t)|. \qquad (3.35)$$

The dynamics of $\dot{s}(\underline{x},t)$ are required so (3.9) can be differentiated with respect to time to get

$$\dot{s}(\underline{x},t) = \ddot{x} - \ddot{x}_d + \lambda\dot{e}. \qquad (3.36a)$$

Then by substituting (3.31) into (3.36a) we obtain

$$\dot{s}(\underline{x},t) = f(\underline{x},t) + b(\underline{x},t)u(,t) + p(t) - \ddot{x}_d + \lambda\dot{e} \qquad (3.36b)$$

where $f(\underline{x},t)$ and $b(\underline{x},t)$ are as described in (3.32) and (3.34) respectively. The system is stable if $s(\underline{x},t)$ converges to zero, which can be assured if $u(\underline{x},t)$ is chosen to satisfy (3.13). The total control consists of two parts (as in (3.24)), one for the known or estimated part of the dynamics ($\hat{u}$) and the other for the uncertain or nonlinear part ($\bar{u}$). Assuming initially that there is no uncertainty in either the control matrix ($b(\underline{x},t) = \hat{b}(\underline{x},t)$) or the transition matrix ($f(\underline{x},t) = \hat{f}(\underline{x},t)$) and that there is no external perturbation present ($p(t) = 0$), then, for this example, the known control is obtained by setting (3.36b) to zero so that

$$\hat{u}(\underline{x},t) = -(1/\hat{b}(\underline{x},t))[\hat{f}(\underline{x},t) + \lambda\dot{e} - \ddot{x}_d]. \qquad (3.37)$$

This control law does not yet satisfy the stability criterion because $f(\underline{x},t) \neq \hat{f}(\underline{x},t)$ and the perturbations $p(t)$ have not been accounted for. The complete control law will have another term $(\bar{u})$ that is discontinuous across the surface in order to satisfy $s\dot{s} \leq -\eta|s|$. Now with all the uncertainties included, where $\dot{s} = \dot{s}(X,t)$, $\dot{s}$ becomes

$$\dot{s} = \hat{f} + \Delta f + \hat{b}u + p - \ddot{x}_d + \lambda\dot{e} \qquad (3.38)$$

and, after substituting $u = \hat{u} + \bar{u}$ into $s\dot{s}$, it becomes

$$s\dot{s} = [\Delta f + p - \bar{u}]s \leq -\eta|s|. \qquad (3.39)$$

This results in $\bar{u} = -k(\underline{x},t)\,\mathrm{sgn}(s)$ so that

$$u(\underline{x},t) = \hat{u}(\underline{x},t) - k(\underline{x},t)\,\mathrm{sgn}(s) \qquad (3.40)$$

where $k(\underline{x},t)$ is determined from the bounds on the uncertainties and perturbations previously estimated as

$$k(\underline{x},t) = [F(\underline{x},t) + P(t) + \eta]. \qquad (3.41)$$

This variable $k(\underline{x},t)$ is the mechanism by which the system uncertainties are accounted for and which will cause the discontinuous part of the control to compensate for their effect. This also insures that $s^2(\underline{x},t)$ is a Lyapunov function which in turn guarantees stability.

If the control gain is also uncertain, then the control must be changed to

$$u(\underline{x},t) = [\hat{u}(\underline{x},t) - k(\underline{x},t)\,\mathrm{sgn}(s)]/\hat{b}(\underline{x},t) \qquad (3.42)$$

where the discontinuous term now is

$$k(\underline{x},t) = B[F(\underline{x},t) + P(t)] + (B-1)|\hat{u}(\underline{x},t)| \qquad (3.43)$$

and B is as defined in (3.34) [Ref. 5]. Again notice that the control discontinuity has become larger to overcome the increased uncertainty in the system.

This discontinuity causes a chattering problem which is present due to the abrupt nature of the sign function, so a smoothing operation needs to be implemented. This can be done by replacing the sign function with a saturating function which has a user defined slope or boundary layer between the upper and lower limits of plus and minus one. This provides a linear region around the surface boundary and smooths the control action (see Figure 5a and 5b). Now the designer has another variable to use, ϕ (called the boundary layer thickness and whose magnitude depends on the level of system uncertainties), along with λ to incorporate into his design. These variables can be made time-varying to account for times when the uncertainties increase or decrease, thus increasing overall performance. [Ref. 6]

The questions of rigorous mathematical uniqueness, existence, and continuability have been addressed in Reference 5 and Reference 7. Though bang-bang controllers are attractively simple and optimal control specialists have pretty much perfected their use, the problem is that the differential equations governing their use have discontinuities on the right hand sides. Therefore, normal uniqueness and existence theory for differential equations no

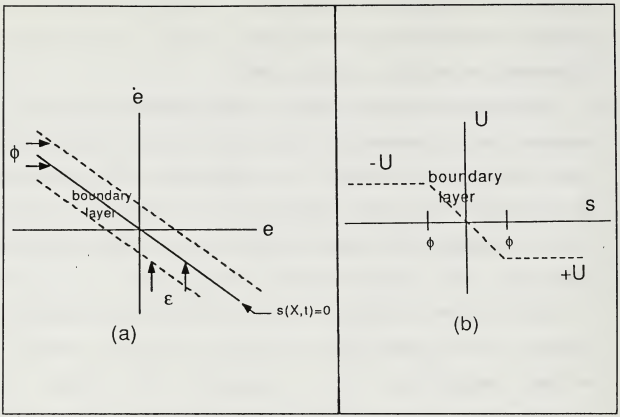

Figure 5 Boundary Layer [After Ref. 5]

longer applies. Filippov proves the existence and continuability for his own solution concept [Ref. 7]. For the question of uniqueness, it can be shown that, by satisfying (3.13), only one solution to the discontinuous differential equation can apply at any given time [Ref. 5]. This is equivalent to saying that the derivative of the state trajectory must always point towards the sliding surface. Although VSC in itself is a powerful design methodology, incorporating an adaptive portion can increase the robustness and performance of the controller.

E. VSC WITH ADAPTIVE COMPENSATION

With the linear model developed in Chapter II, we will now determine a simple adaptive controller capable of tracking the state of a reference model in the presence of uncertainties in the AUV dynamic parameters. The state space description of this model is

$$\dot{\underline{x}}(t) = A\underline{x}(t) + \underline{b}d(t) + \underline{f}(x) \qquad (3.44)$$

where d(t) is the control input and f(x) is the nonlinearity which comprises model inaccuracies, external perturbations and changing parameters. This depth controller design is based on the model dynamics with an adaptive loop to place the eigenvalues for the desired linear part and a switching input based on VSC design for the nonlinear part f(x). The controller should drive the AUV to a desired depth z_d and keep it there, despite system uncertainties and external disturbances. The difference between the actual state $[q,\Theta,z/(-v)]'$ and the desired state $[0,0,z_d/(-v)]'$ (where v is the vehicle speed) is defined as the error state

$$\underline{e}(t) = [q,\Theta,(z-z_d)/(-v)]'. \qquad (3.45)$$

Due to the presence of integral action in the vehicle model (3.44), we can include the constant desired depth in the initial condition of the integrators and write (3.44) with $\underline{e}$ as the state (rather than $\underline{x}$).

Now let us choose a model matrix A_m with eigenvalues determined by the desired closed loop response. Clearly A_m

has eigenvalues in the stable region. If we choose A_m such that the pair (A_m,b) is in controllable canonical form, then it is a simple exercise to show that the vehicle dynamics (3.44) can be written as

$$\dot{\underline{e}}(t) = A_m\underline{e}(t) + \underline{b}(d(t) + \underline{K}'\underline{e}(t)) + \underline{f}(\underline{e}) \qquad (3.46)$$

where the vehicle dynamics (at the current operating conditions) determine the required gain $\underline{K}$. This dynamic model (3.46) is at the basis of an adaptive controller which will drive the error state $\underline{e}(t)$ to zero and track the ordered depth. The surface $s(\underline{e}) = 0$ is defined (as described in (3.9)) as a linear combination of the error states, namely

$$s(\underline{e})=c'e(t). \qquad (3.47a)$$

For this particular formulation, let $\underline{c}'$ be the left eigenvector of the matrix A_m associated to any of its stable eigenvalues, $-\lambda$(i.e., $\underline{c}'A_m = -\lambda\underline{c}'$). By the fact that A_m is in companion form by assumption, it is possible to show [Ref. 8] that the entries of the vector $\underline{c}'$ are the coefficients of the polynomial having all other eigenvalues of A_m as roots. Since $q=\dot{\theta}$, $\theta=\dot{z}$ and z_d is constant, we can write $s(\underline{e})$ as

$$s(\underline{e}) = c_2e^{(2)} + c_1e^{(1)} + c_0e \qquad (3.47b)$$

where $e=(z-z_d)/(-v)$, and $\underline{c}'=[c_2\ c_1\ c_0]$. All this implies that the surface $s(\underline{e})=0$ satisfies one of the requirements of being a sliding surface, i.e.,

$$s(\underline{e}) = 0 \Rightarrow \lim_{t\to\infty} \underline{e}(t) = 0 \qquad (3.47c)$$

On the basis of this definition we can determine an adaptive controller which drives the state error $\underline{e}$ onto the surface $s(\underline{e})=0$ as follows.

In the model (3.46) let us assume that bounds

$$K_i^{min} < K_i < K_i^{MAX} \tag{3.48}$$

on the entries of the vector K, and a bound

$$F(e) > |c'f(e)/c'b| \tag{3.49}$$

on the nonlinearities are known to the designer. Then, under this assumption, the control input is

$$d(t) = -\underline{K}'(t)\underline{e}(t) + F(\underline{e})\mathrm{sgn}\{s(t)\} \tag{3.50}$$

with $\hat{K}$ the adaptive gains defined as

$$\dot{\hat{K}}(t) = -\sigma\{\hat{K}(t)\} - \mu e(t)s(t). \tag{3.51}$$

The expression $\sigma_i\{\hat{K}(t)\}$ is given by

$$\sigma_i(\hat{K}(t)) = \begin{cases} 0 & \text{if } K_i^{min} < K_i < K_i^{MAX} \\ -\alpha(\hat{K}_i(t) - K_i^{min}) & \text{if } K_i(t) < K_i^{min} \\ -\alpha(\hat{K}_i(t) - K_i^{MAX}) & \text{if } K_i(t) > K_i^{MAX} \end{cases} \tag{3.52}$$

(where α is a positive constant), hence (3.51) yields a closed loop response which is exponentially stable and $\underline{e}(t) \rightarrow 0$. [Ref. 4]

Proof: Using the fact that $\dot{s}=c'\dot{e}$ and $c'A_m=-\lambda c'$, we can write (3.46) from (3.47) and (3.50) as

$$\dot{s}(t) + \lambda s(t) = c'b\bar{K}'(t)e(t) + c'f(e) - c'bF(e)\mathrm{sgn}\{s(t)\}, \tag{3.53}$$

where $\bar{K} = \hat{K} - K$ is the parameter error. Define the Lyapunov function as

$$V(s,\bar{K}) = 0.5(s^2 + g\bar{K}'\bar{K}) \tag{3.54}$$

where $g = c'b/\mu$ (a positive quantity). The time derivative of (3.54) is

$$\dot{V}(s,\underline{K}) = -\lambda s^2(t) - c'bF(e)|s(t)| + c'f(e)s(t)) \\ -g\underline{K}'(t)\underline{\sigma}\{\hat{\underline{K}}(t)\}. \qquad (3.55)$$

Now we can see that the term $\underline{K}'(t)\underline{\sigma}\{\hat{\underline{K}}(t)\}$ is always nonnegative by definition of the function $\underline{\sigma}(\hat{\underline{K}}(t)) = [\sigma_1(\hat{K}(t)),\cdots,\sigma_n(\hat{K}(t))]'$ in (3.52). Also, by the definition of the bound $F(\underline{e})$ on the nonlinearity, the term $\{c'bF(e)|s(t)| - c'f(e)s(t)\}$ is always nonnegative. Therefore

$$\dot{V}(s,\underline{K}) \leq -\lambda s^2(\underline{e}(t)) \leq 0 \qquad (3.56)$$

along the trajectories of the system. This implies that $s(\underline{e}(t))$ is always bounded and also that the adaptive gains $\hat{\underline{K}}(t)$ are bounded. This, combined with (3.56), yields

$$\lambda\int_0^{+\infty} s^2 dt \leq -\int_0^{+\infty} \dot{V}(t)dt \leq V(0)-V(\infty) < \infty \qquad (3.57)$$

from which we deduce that

$$\lim_{t\to\infty} s(\underline{e}(t)) = 0 \qquad (3.58)$$

and $\underline{e}(t) \to 0$, which proves the result.

F. SIMULATIONS AND RESULTS

The controller (3.50) has been implemented in MATLAB and the basic flow chart is outlined in Figure 6. The performance is satisfactory at all speeds and, depending on the desired closed loop eigenvalues (i.e., the choice of the matrix A_m), the response could be tailored towards minimum rise time or minimal overshoot. While we used a saturation function instead of a sign function in our program, our process achieves

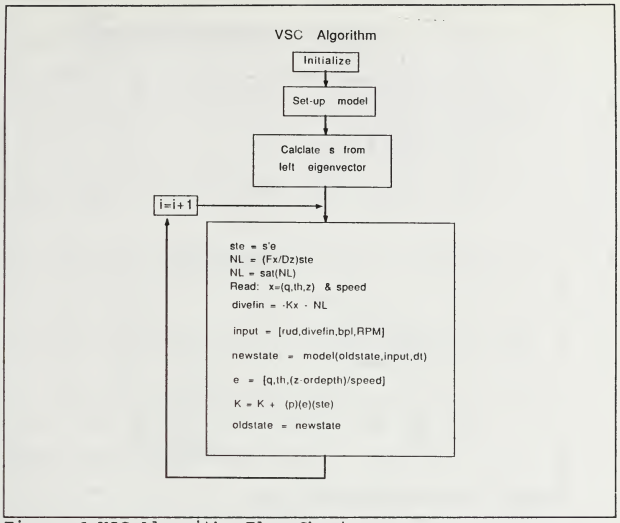

Figure 6 VSC Algorithm Flow Chart

further smoothing of the discontinuous boundary by use of the integral process in determining the feedback gains K_i. The simulation results are shown in Figure 7 while Figure 8 shows a plot of typical feedback gains.

These results show that the controller performs satisfactorily over a wide range of operating conditions, ranging from 100 to 500 rpm of the thrusters. The different rise times appearing in the depth plot in Figure 7 are consistent with the different speeds of the vehicle. In all

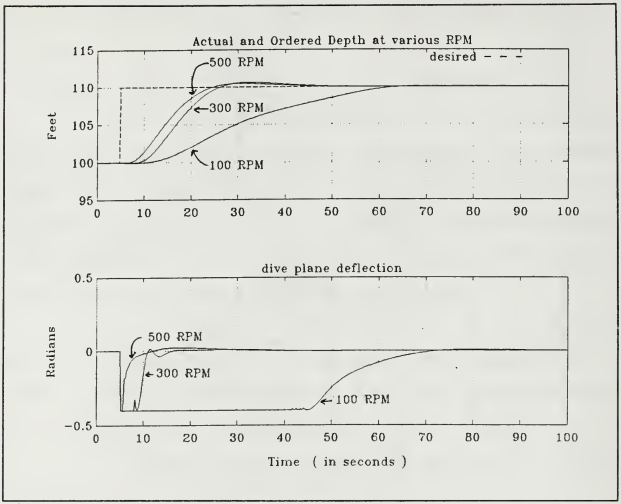

Figure 7 VSC Performance Plots

three runs the dive plane action (bounded within ± 0.4 radians, or ± 23 degrees due to the physical constraints) does not show any chattering due to the linear saturation adopted for the controller (3.50), rather than the sgn function formulated in the theory. The result is a smooth operation of the dive fin (stern plane).

The adaptive gains K_1, K_2 and K_3 plotted in Figure 8 stay within reasonable values and converge to constants which depend on the operating conditions. The surface S is also

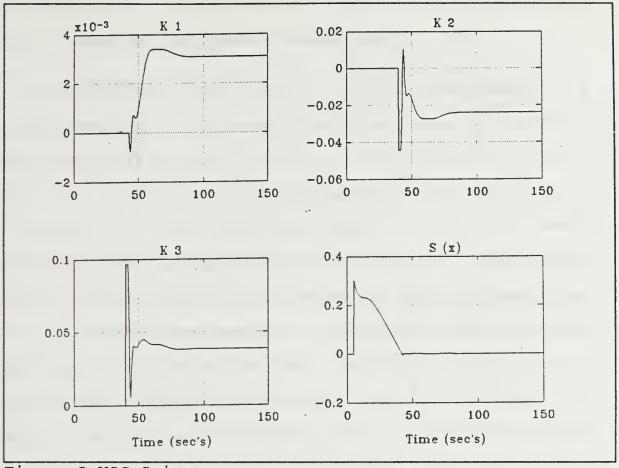

Figure 8 VSC Gains

plotted and is shown to be driven to zero and kept there. For these particular plots the speed of 300 rpm is assumed.

Considering the simplicity of the controller, we could conclude that this control scheme is satifactory for on-line implementation on the AUV under development at NPS. Although the VSC method is an efficient nonlinear design method, other linear design schemes are available which can also satisfy the robustness requirement.

IV. LINEAR ROBUST CONTROL OF THE AUV

A. INTRODUCTION

The VSC described in the previous section has been shown to exhibit satisfactory robustness properties in the presence of nonlinearities and unmodeled dynamics. A major requirement, however, of VSC is that the states must be available for measurement. For the AUV on a dive maneuver this is not much of a drawback since the state signals (pitch rate, pitch and, depth) are provided by gyros and the depth cell.

There are situations, however, in which we might want to be able to control the vehicle with incomplete state information. This is the case when it is important to provide for reliability in the sense of ensuring the success of the mission, even in the presence of failure of a gyro or its circuitry. In these cases a model based on an observer provides for the missing measurements by estimating them from the other available signals.

It is a well known fact that robust design techniques based on full state feedback are bound to lose their robustness properities when the state is replaced by an estimate from an observer. This has been pointed out by Doyle-Stein [Ref. 9] in the context of robust linear controllers. In the next section we introduce the notion of robust observers designed to preserve the robustness properties of

the compensator. The performance of the AUV with this type of observer is given in the last section.

B. ROBUST OBSERVERS AND THE DOYLE-STEIN CONDITION

The design of a compensator usually starts with a system description such as

$$\dot{x} = Ax + Bu \tag{4.1a}$$

$$y = C'x + Du \tag{4.1b}$$

where **A** is the plant transition matrix, **B** is the control matrix, **C** is the observation matrix, and **D** is the feedthrough matrix (usually it is zero). Because of the Separation Principle, the controller and observer can be designed independently. Designing the controller is usually the first step and starts with finding the gains of the feedback control law (u=-Gx) where the required response is determined from system specifications. The gains are then selected by a pole-placement formula such as the Bass-Gura method or Linear Quadratic Regulator (LQR) methods, based on a quadratic performance index, and hence solve a Riccati equation associated with the system (4.1). Real life constraints on the physical system limitations (such as the power supply) limit the size of the control **u**, and this limitation can easily be imbedded in an LQR design.

When all state signals are not available for measurement, an observer provides for their estimates from input/output measurements. Using a Luenberger observer of the form

$$\dot{\hat{x}} = A\hat{x} + Bu + K(y-C'\hat{x}) \qquad (4.2)$$

it is well known that $x-\hat{x} \rightarrow 0$, provided A-Kc' has stable eigenvalues. With the observer, the control input becomes $u=-G\hat{x}$. The use of an estimated state (rather then the state itself) might seriously affect the robustness of the controller. Even the seemingly sensible solution of making the estimated state $\hat{x}$ converge to the actual state x as fast as possible (i.e., decrease the negative real part of the eigenvalues of A-Kc') does not, in general, improve robustness of the closed loop system [Ref. 9].

A significant problem concerning a lack of robustness (i.e., sufficiency of the gain and phase margins in the presence of parameter variation) has been associated with systems whose observers were designed solely on the assumed sensor noise parameters [Ref. 10]. Therefore, the issue of robustness of the closed loop dynamics should be investigated as part of the design process of an observer. A typical LQR controller using full state feedback can have gain and phase margins well in excess of six decibels and 60 degrees respectively; however, using an observer, the margins can be reduced significantly (refer to Figure 9). The effect of using faster observer poles is shown in Figure 9. In this example (taken from [Ref. 9]) the Nyquist plot of the system with full state feedback is compared with the plot of the same controller with observed state feedback. The optimal filter

(a steady state Kalman filter) and an observer with "fast dynamics" have the effect of greatly diminishing the stability margins of the system. [Ref. 9]

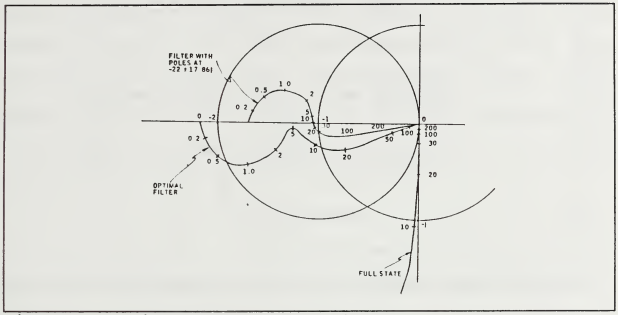

Figure 9 Nyquist Plots [From Ref. 9]

Consider the two systems in Figure 10 where both systems are minimum phase, observable and controllable. For comparison, the controller sections have been highlighted by placing them inside the dashed lines. Many of the possible transfer functions have been compared and investigated with regard to robustness from the connections marked X and XX. It has been shown that the closed loop transfer functions from r to x are identical along with the loop transfer functions (with the loops broken at XX) from u' to u. Yet the loop transfer functions (with the loops broken at X) from u" to u' are not the same in the two systems unless the relationship

$$K[I + C(SI - A)^{-1}K]^{-1} = B[C(SI - A)^{-1}B]^{-1} \qquad (4.3)$$

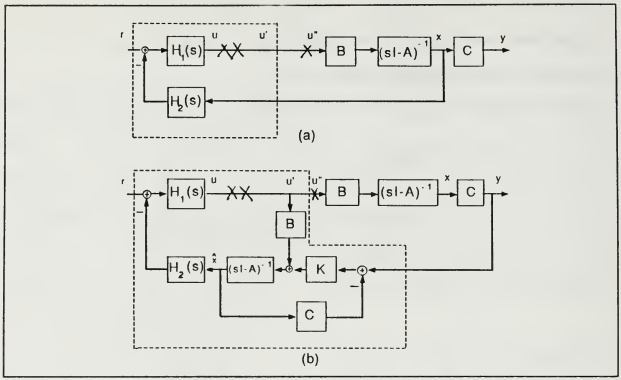

Figure 10 Feedback (a)Full-State (b)Observer [After Ref. 9]

holds. Recall that **K** is the observer gain which now has certain restrictions placed on it from (4.3). This relationship is known as the Doyle-Stein (D-S) condition, is independent of the control gain and depends only on the open-loop characteristics of the observer. When (4.3) holds, the observer does not influence the transfer function from r to x [Ref. 10]. Finally, note that the loop transfer functions are the same only at point XX, which is inside the designed controller, but they are not the same at point X, which is the control interface to the plant and where natural parameter uncertainties will most probably occur. [Ref. 9]

Doyle and Stein have shown that, if the observer gains are parameterized as a function of q (a scalar variable), then

this particular function K(q) must meet certain requirements as $q \to \infty$ with the main one being that

$$K(q)/q \Rightarrow BZ \tag{4.4}$$

where Z is any non-singular matrix [Ref. 9]. A Kalman filter provides for such a function (one of many possibilities) that works for all controllable, observable and minimum phase systems. This is similar to assuming that the covariance Q of the process noise used in the Kalman filter has the special form of

$$Q(q) = Q_o + q^2 BWB' \tag{4.5}$$

where W is any positive definite symmetric matrix and q is the scalar weighting factor defined above. (The value q=0 is associated with the nominal steady state Kalman filter gain for the assumed process noise Q_o.) As $q \to \infty$, the response tends toward the full state feedback response as shown in Figure 11. The extra term in (4.5) is equivalent to adding extra process noise to the control input of the plant. Normally q is increased until a satisfactory compromise between robustness and noise performance is obtained. This method gives an easy way to balance the requirement between noise rejection and stability margins. We have investigated this method with regard to the NPS AUV vehicle model and present the results in the next section. [Ref. 9]

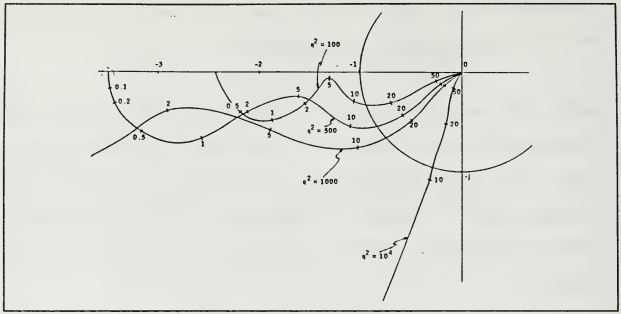

Figure 11 Fictitious Noise Nyquist Plots [From Ref. 9]

C. SIMULATIONS AND RESULTS

Following the background development of a Doyle-Stein observer (robust observer) that was presented in Chapter II, we first need to generate numerical values for the linear model of the AUV. Presently, there are many simulation languages available, but we used MATLAB. The complex and large C program that encompasses the AUV model was implemented as a function in MATLAB. This allowed us to try many forms and types of controllers and to simulate them in a much easier fashion than a conventional language might have afforded. Mainly this was because of the rich libraries and simple graphics that MATLAB has and the relative ease of changing and modifying the algorithms of the controller.

The AUV model can be fit to an ARX (AutoRegressive) discrete time model of

$$A(q^{-1})y(kT) = B(q^{-1})u(kT) + e(kT) \qquad (4.6)$$

where **A** and **B** are polynomials in the time delay operator q^{-1}, **T** is the sampling interval and **e** is an error sequence (possibly colored). Using this ARX model and a Recursive Least Squares (RLS) or Recursive Instrumental Variable (RIV) algorithm, the parameters of the model can be estimated. In general the RIV methods are better suited to cases when the noise is significantly colored (non-white). In our case, a third-order model has been estimated using both RLS and RIV with only small differences noted in the numerical results. The input to the RLS algorithm is required to be "persistently exciting" so that all modes of the model will be excited.

Since a fourth order model yields very similar results, the choice went to the simpler third order model, further confirming the model choice made in Chapter II. Figure 12 is a plot of the input, actual output and estimated output.

The next step was to generate the state feedback and estimator gains. MATLAB functions were used extensively in this area. For state feedback any pole placement techniques will work such as DLQR or PLACE in MATLAB. We used the steady state Kalman gains from DLQE for the estimator gains where the process noise was adjusted or modified according to equation (4.5). Copies of the MATLAB programs used in this thesis can be obtained by contacting Professor Roberto Cristi (fourth entry in the initial distribution list, phone 408-646-2223).

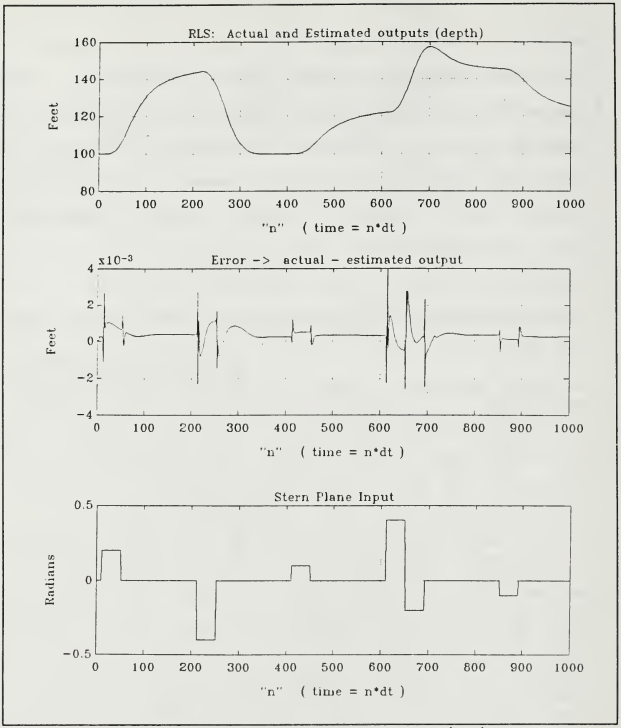

Figure 12 RLS Model Input/Output Characteristics

Figure 13 shows the performance of the controller for several choices of robust observer. As outlined in the previous section, the robust design yields a family of observers (parameterized by the parameter q) which improve robustness as q becomes larger. This effect is shown in Figure 13, where the depth responses obtained with q=0, 10 and 50 are shown. Notice the increased stability and reduction of oscillations. This is also shown in the input signal which is limited to ± 0.4 radians.

Regardless of the type of controller used (VSC or robust observer), an efficient implementation in hardware requires at least a survey of the available AUV architectures.

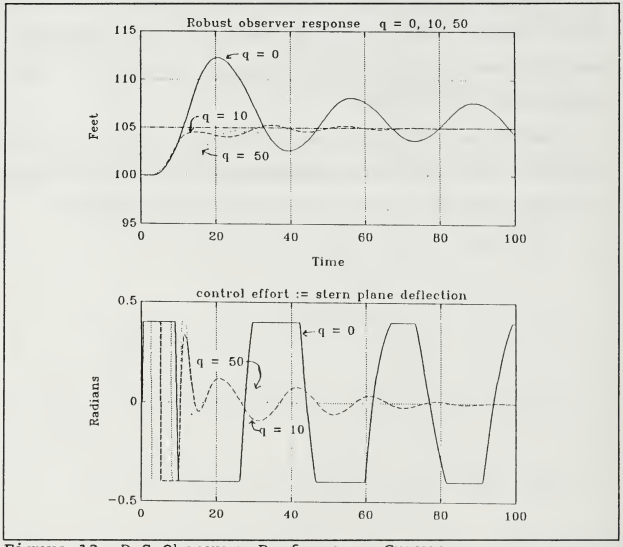

Figure 13 D-S Observer Performance Curves

IV. AUV ARCHITECTURE

A. INTRODUCTION

AUV systems and their related hardware have become increasingly complex in order to satisfy all the levels of vehicle control. These levels encompass varying degrees of asbtraction from the highest (Artificial Intelligence) to the lowest (actuator control algorithms). Historically, the challenge has been to find some sort of hardware and software combination to satisfy all the constraints generated by such a sophisticated system. The problem is that a general purpose microcomputer solution tends to be slow (non-real time) and inefficient or non-optimal. The trend is to "tailor" the hardware and software to the problem at hand. This "application specific" approach is especially germane with robotics and AUV systems since they rely heavily on sensory feedback where real-time response is a necessity. Most of the systems surveyed were set up in some sort of hierarchical fashion corresponding to the various levels of "intelligence" or abstractions in their mission plans. Each level has its own numerical computational requirement; therefore, hardware and software selections for each level must be tailored for that specific application. This should allow the system to be as efficient as possible and to allow the lowest control level to run in real-time. This chapter looks at some of the

various hardware methods which can help achieve this real-time performance requirement at the control-actuator interface and yet still allow some flexibility in design which will encompass a wide range of applications.

A. HARDWARE ALTERNATIVES

The architecture specifications should match or exceed the performance requirements of the algorithm which are normally formulated in terms of latency (elapsed time from when the input is present until the output is ready) and throughput rate (given in MIPS or MFLOPS). There is a tendency to concentrate on the throughput performance while the latency (i.e, delay) is of critical importance in control algorithms (the system stability requirements may allow only so much inherent delay). Control applications normally require positional accuracy, concurrent tasks, repeatability, robustness and timing constraints (tasks must all be done within the sampling period) for the hardware. It seems reasonable that the optimal approach would be some combination of the various hardware technologies. Some of these technologies are:

- pipelining,
- RISC (Reduced-Instruction-Set-Computer),
- bit-sliced microprocessors,
- vector processing,
- DSP (Digitial Signal Processing) chips,

- ASIC (Application-Specific Integrated Circuit) chips,
- systolic arrays,
- multiple processors, and
- PLDs (Programmable Logic Devices). [Ref. 11]

Pipelining (paralleling the datapath) tries to improve the throughput by shortening the clock cycle, but then the latency also increases. The concept will also work well at higher levels of control or abstraction (concurrent programming) and not just at the computational level such as a multiplier/accumulator (MAC). [Ref. 11]

RISC is a diverse technology and is still subject to much debate and company specific design philosophy. The performance comes from using less "chip real estate" to encode fewer instructions thus leaving more room to add additional components to speed up overall program execution. Several manufacturers have working RISC microprocessors and their throughput performance is impressive. RISC systems have not had many commercial applications because twice as much memory (versus a 80X86 system) is required and their speed advantage has eroded since the newer 80X86 chips are much faster now. Even so, AUV control is an area where a dedicated RISC architecture might be exploited in a generic controller scenario.

Bit-sliced microprocessors are very fast since they generally use an ECL (Emitter-Coupled-Logic) chip set. They

can be tailored to an individual application and fit very well into fault tolerant systems. Their power hungry ECL construction and multi-chip expense limit their general use in a space and energy conservative environment such as an AUV, but certain performance constraints requiring ultra fast processing would benefit from their use. [Ref. 12]

Systolic arrays and vector processing basically combine several arithmetic or processing units in various geometries to improve the data stream flow. The general idea is to increase performance by some sort of parallel computation. Most of the supercomputers use some form of vector processing to achieve enormous throughput capability and systolic arrays have been used fairly successfully in image processing systems. The multi-dimensional nature of an AUV system along with the MIMO control problem (with its discrete time dynamical difference equations) requires a matrix formulation and then a real-time solution which lends itself to this type of processing.

DSP chips have begun to flourish and their performance is truly remarkable. Several of the well-established companies that market 32-bit floating point processors are: Motorola (DSP96002), Texas Instruments (TMS320C30) and AT&T (DSP32C-80). While the state-of-the-art DSP chips are relatively expensive, their performance (33 MFLOPS for the T.I. chip), onboard memory and on chip I/O make them virtually a single

chip solution for almost any control or filter problem. The capability of extensive on-chip programming and the ability to move blocks of memory onto the chip greatly enhances the actual throughput of a large control algorithm. A possible pitfall with these chips is that along with the substantial performance increases come commensurate leaps in system details (debugging programs, etc.). The most effective way to minimize this problem and its learning curve is to purchase the complete package (C compiler, PC-board, etc.) from the manufacturer. Here again it is probably best to stay with well-established companies who are marketing their next generation chip which already has most of the required software available from the previous generation's chip product line. The final choice of DSP chip will be a balance between performance, cost and supporting software (which is the most important item considering the essentially equivalent performance from all of the 32-bit chips). The time and effort involved in getting any DSP chip to actually work in a system will entail a large portion of the total resources, so any product that can shorten or automate this process will be money well spent.

The term ASIC seems to suggest that it is a combination of some design methodology, system requirements and choice of algorithm which, taken collectively, purport to solve some specific control problem. This would allow many of the system

overhead functions usually performed by a general purpose microprocessor to be eliminated, and hence an overall performance increase would be achieved. ASIC devices typically are either full custom or semi-custom with the latter the most common due to the greatly reduced design costs. Semi-custom designs normally use gate arrays or standard cells (gates, registers, ALU, etc.) with the former the most popular since it generally has a faster design turn around time. A natural application for these chips would be in an AUV system where navigation, actuator controllers and sensor processing could require vast computational power. Generally the problems to be addressed are testability of the ASIC design and efficient layout (interconnections) of the chip to minimize propagation delays. [Ref. 13]

One of the more exciting areas to explore is that of multiple processors. There are various methods and ideas on how to implement these distributed computing techniques. One of the more important decisions is the one between message passing and shared memory. Message passing can have a long latency time and a large overhead due to protocol requirements. The allure of multiple processors is that the type of processor used can be chosen to best complement the particular algorithm at hand. How the inter-communications between processors is handled is a crucial design decision second only to the processor choice itself. [Ref. 11]

There are essentially only a few methods of inter-communication between processors: RS232 cable, a local or system bus, shared memory (dual port RAM, etc.) or a local area network (LAN) line (e.g., Ethernet). The LAN tends to have a lot of overhead, is serial in nature and, hence, is relatively slow. For distant processors that need infrequent communications this could be a viable method, but for tightly-coupled processors a versatile bus is the only real choice. There are several styles and types of buses from which to choose; they range from simple passive backplanes to forward-looking high-speed 32-bit buses. Issues such as compatibility and performance must be investigated and the inevitable compromises made. Several types of buses can be employed in one system since AUV control systems tend to be hierarchical in topology and each layer of control or abstraction can be tied together with a particular bus to fulfill a specific need.

The newest 32-bit buses offer the most performance and versatility so far. They can block transfer to RAM, do cache coherence, autoconfigure (poll boards attached to the bus and then adjust the related interface software) and interact with the fault-tolerant system (i.e., logically remove the faulted board on-line). Some of the buses can handle larger bus widths of up to 256 bits of data (e.g., FUTUREBUS+ : IEEE standard P896). The U.S. Navy has decided to base all

mission-critical computers on FUTUREBUS. Given this decision and the superb performance and adaptability of this bus, it would seem a natural choice for future expansions. Of special note is the new type of transceiver used by FUTUREBUS called BTL (Backplane Transceiver Logic). This transceiver reduces the bus capacitive load and hence increases the bus bandwidth to 400 Mbytes/sec (an order of magnitude better than ECL transceivers). [Ref. 14]

Finally, PLDs of which the EPROMs and PALs are examples are a relatively cheap way to implement functions or processes. PLDs are expandable, universally compatible and, by design, tailor-made to the specific application and algorithm. These devices are cheap (compared to DSP devices) and several versions are in development that have provisions to be re-programmed on the fly (EEPROMs, etc.).

B. OPERATING EXAMPLES

While there are as many theories and ideas on how an AUV architecture should be built as there are AUV manufactorers, it can be quite helpful to investigate a few designs which have been built and are actually operational. This section will briefly overview three vehicles:

- ARCS (Autonomous Remotely Controlled Submersible) built by International Submarine Engineering Limited (ISE) in Canada.
- EAVE (Experimental Autonomous Vehicle) EAST built by the University of New Hampshire.

- FS (Free-Swimmer and formally EAVE WEST) built by Naval Ocean Systems Center in San Diego, CA.

Table 1 is a partial list of several AUV designs and their ROV manufacturers. Two comprehensive AUV references that detail current vehicles are ROV Review 1990 and Undersea Vehicles Directly 1990. (ROV Review can be purchased after January 1990 by contacting Dean Given, PO Box 368, Spring Valley, CA 92077, phone 619-660-0402. Undersea Vehicles Directory can be purchased after November 1989 by contacting Frank Busby in Arlington, VA, phone 704-892-2888.) [Ref. 15]

The ARCS is a commercially available AUV, so it uses "off-the-shelf" hardware and software to reduce costs. The modeling of the control system organization followed that of a typical naval submarine and a multi-tasking setup was used to schedule all the tasks. The specific hardware included a 16-bit CPU for the multi-tasking, an Intel Multibus and three single board computers (two 8086s with 8087s and one 8088), tied together with a common backplane bus and sharing some dual port RAM. Interfaces to external equipment were through RS-232 serial links. The requirements for a real-time multi-tasking operating system led ISE to choose Intel's RMX86 system. [Refs 16 and 17]

The University of New Hampshire has been developing and enhancing their AUV project since 1977. They are currently pursuing their third generation vehicles which stress Artificial Intelligence (A.I.) concepts and multi-vehicle

cooperation. EAVE EAST III has much greater memory capability and processing power than its predecessors in order to serve as a testbed for future concepts and evaluations. Their computer system is hierarchical with three distinct levels. The lowest level handles all the fast (less than one second) systems including reading sensors, pre-processing data and controlling actuators. This level consists of three 68000 processors which communicate over RS-232 cable to each other and to an interface with the higher levels. This lower level can control the vehicle without any higher level assistance.

The higher level architecture consists of several 68020 processors on a VME bus and liberal use of dual port memories which allow local CPU use as well as communication by other CPUs on the bus. Figure 14 shows this multi-bus setup which helps to incorporate I/O and data storage into the overall system. Their choice of a real-time operating system was pSOS which was also tasked with running a symbolic language (LISP). So far their choice of architecture, hierarchy and software has proven to be reliable, capable and extensible. [Ref. 18]

NOSC has a wealth of experience in underwater vehicles and their subsystems. Their FS (Free-Swimmer or previously known as EAVE WEST) vehicle has been through several upgrades in capability. Although it is probably not as advanced as some of their current vehicles (which have restricted distribution due to assigned mission areas), FS should be

Table I Current AUVs [From Ref. 15]

Vehicle	Depth, meters	Developer	Comments
Advanced Underwater Vehicle (AUV)	NA	U S. Defense Advanced Research Projects Agency, Washington, D C.	Project to develop low-drag vehicle, apply aerospace technology to control functions; program completed in 1984, prototype was smart, guided torpedo under development by Rockwell International. Investigated suction techniques for drag reduction
Advanced Unmanned Search System (AUSS)	6100	U S. Naval Ocean Systems Center (NOSC), San Diego, Calif.,	A 4 3-meter vehicle undergoing shallow water tests; some problems to date with transmitting data through water. Intent is to achieve 4800 bits per second from 6000 meters; developed for search and identification
Buoyancy-control unit	300	United Technologies' Hamilton Standard Division, Windsor Locks, Conn	Demonstration vehicle, automatic control uses compressed air to vary water ballast, no horizontal capability, sea tests began in 1983
Autonomous remotely controlled submersible (ARCS)	300	International Submarine Engineering Port Moody, B C., Canada	Developed for under-ice mapping, successful under-ice sea trials in late 1984; 4 4 meter vehicle capable of 5 knots for 20 hours, controllable to 8 km at 30 meter depth
Autonomous Underwater Vehicle (AUV)	NA	Hydro Products, San Diego, Calif., and its parent Honeywell, Seattle, Wash	Internally funded program, still in early stages, to develop modular vehicle with unique target recognition and homing sensors, first tests planned for 1986
B-1	100	U S. Naval Underwater Systems Center, Newport, R I	A 2.7-meter teardrop vehicle designed for optimum shape for laminar flow, over 50 runs, records 52 channels of performance data
Control System Test Vehicle (CSTV)	NA	U S. Naval Coastal Systems Center (NCSC), Panama City, Fla	A $\frac{1}{4}$, model submarine 9 meters long, uses Kalman filter integrated navigation comprised of ring laser inertial navigation unit, acoustic range system and various speed sensors, low telemetry link, real-time onboard control, top speed 15 knots, more than 20 tests in Gulf of Mexico demonstrating high maneuverability, but none since September 1983
CMU Rover	0	Carnegie-Mellon University Pittsburgh, Pa	Project supported by U S. Office of Naval Research to develop intelligent self-navigating robot with stereo vision and sonars for obstacle avoidance
EIR	1000	Institut Francais de Recherches pour l'Exploitation de la Mer (Ifremer) and Comex Industries Toulon, France	$7 5 million project underway to develop vehicle by 1987 with real-time acoustic speed of 2 knots, for inspection use on surveys and around offshore oil platforms
Experimental Autonomous Vehicle East (Eave East)	900	University of New Hampshire, Durham, N H	A 1 5 meter box-like autonomous vehicle test bed for structure and pipeline inspection, numerous lake tests showing obstacle avoidance capability, speed 1 5 knots
Experimental Autonomous Vehicle West (Eave West)	610	U S. NOSC, San Diego, Calif	Experimenis with fiber-optic communication link using cable paid out from each end, wideband TV employed on uplink, subsystem developed to detect and follow pipeline, vehicle speed 5 knots
Epaulard	6100	Ifremer and Societa ECA (Etudes Constructions Aeronautiques), Paris	More than 200 dives since 1979 for seabed photography and bathymetric surveys, controlled acoustically and preprogrammed, more intelligent modal under development
Large Scale Vehicle (LSV)	NA	U S. NCSC, Panama City, Fla., and Sperry Corp., Great Neck, N Y.	To be a one quarter model of new class high speed nuclear attack submarine, autonomous control with telemetry override, unmanned vehicle mainly for propulsion studies but also acoustic and hydrodynamic research; lake tests scheduled for late 1987 near Coeur d Alene, Idaho
Robot	90	Massachusetts Institute of Technology, Cambridge, Mass	A torpedo shaped 2 4 meter vehicle capable of 3 knots, lake tested, part of ongoing student projects but currently inactive MIT was also designing computer-controlled manipulator arm for free swimming vehicle in cooperation with NOSC in San Diego
Rover	300	Heriot-Watt University Edinburgh, United Kingdom.,	A test bed program to develop a structure inspection vehicle that communicates by horizontal acoustic link to tethered vehicle, sea tests planned for early summer
Remote Underwater Mine Countermeasures (Rumic)	NA	U S. NCSC, Panama City, Fla	Prototype undergoing tests to detect and neutralize mines, Doppler sonar navigation system
Skat	NA	Shirshov Institute of Oceanology, Academy of Sciences, Moscow, USSR	Prototype reported to be for ocean research
Self propelled underwater research vehicle III (SPURV III)	1500	University of Washington, Seattle, Wash	A 4 7 meter vehicle operational since its modification in 1979, performs mapping and submarine wake surveillance, also used in tandem with one of two earlier SPURV I vehicles, with one slaved to the other acoustically underwater
Unmanned Free Swimming Submersible	360	U S. Naval Research Laboratory, Washington, D C.	Prototype of program initiated in 1975 to develop high speed search vehicle with range of 1900 km, has undergone shallow water tests, project currently inactive
Unnamed	1000	Thomson-CSF, Brest, France and Comex Industries, Marseilles, France	Prototype for structural inspection and drilling support; several tests, program currently inactive
TM 308	400	Tecnomare Spa, Venice, Italy	Prototype vehicle for inspection and maintenance of offshore oil platforms, diesel powered, teleoperated by acoustic link, manipulator arm, sea tests planned for 1988
Vela	NA	Commissariat a l'Energie Atomique (CEA) and France Dunkerque Shipyard, Paris	Prototype designed for nodule collection

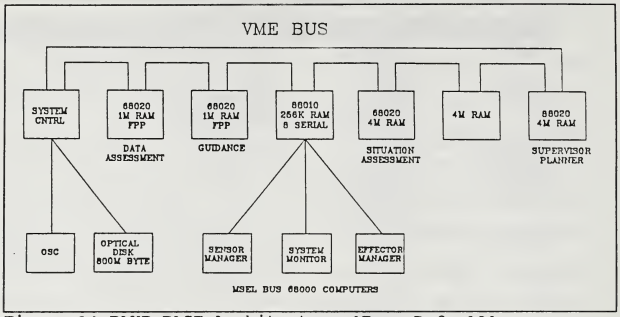

Figure 14 EAVE EAST Architecture [From Ref. 18]

fairly representative of their architectural design philosophy. The NOSC undersea branch is committed to all aspects of AUV-related research from using a transputer array to simulate an Artificial Neural Network (ANN) to designing and testing a Plan Execution System (PES). [Ref. 19]

The FS architecture takes a layered approach as pictured in Figure 15. Their PES runs on an 80286 CPU and communicates with the navigator CPU (8088) and the lower level bus through a RS-232 link. The lower level groups several functions (using 8088 CPUs) together along with sensors and actuator (effector) I/O. Their system requirements lead them to use VERTX for the operating system.

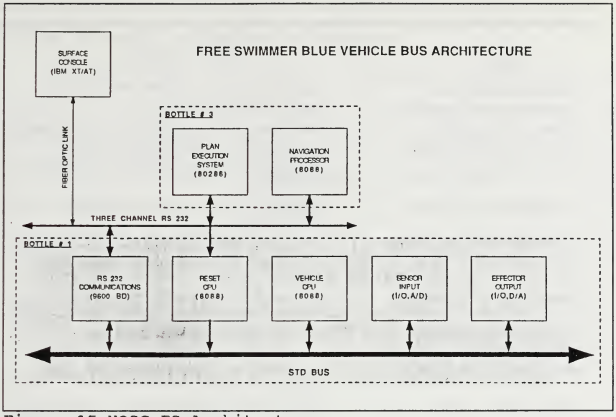

Figure 15 NOSC FS Architecture

This is just a sampling of the current operational AUV architectural designs. Table 2 lists several other organizations and some of their research. [Ref. 12].

D. OBSERVATIONS

The selection of an AUV architecture is a very critical process because the system must be expandable and compatible enough to meet ever-increasing complex missions needs. The design of a generic AUV architecture would entail several key items.

First, the overall system would be hierarchical in nature with several layers of control. This aspect would suggest

Table II AUV Research Organizations [After Ref. 12]

VISITED	PURPOSE/IMPORTANCE
AMETEK-STRAZA/SAN DIEGO	PROVEN CAPABILITIES, TRENDS, WORK SUITES
ARL/UNIV. OF TEXAS/AUSTIN	OBSTACLE AVOIDANCE SONAR
AUTONETICS, LOS ANGELES	NAVIGATION, AOVs, HYDRODYNAMICS, LOW DRAG BODIES
DRAPER LABORATORIES, BOSTON	AUTONOMOUS VEHICLE PROCESSING AND CONTROL, NAVIGATION, RELIABILITY ANALYSIS, LIGHTWEIGHT STRUCTURES
HYDROPRODUCTS, SAN DIEGO	PROVEN CAPABILITIES, TRENDS, UNTETHERED APPLICATIONS
EDO WESTERN, SALT LAKE CITY	SONARS, TV CAMERAS
GOULD, BALTIMORE	ENERGY SUPPLIES, FIBER OPTICS, CABLE HANDLING SYSTEMS
HONEYWELL MARINE, SEATTLE	NAVIGATION, ACOUSTIC LINKS, VEHICLE CAPABILITIES, TRENCHING, MK-50 TORPEDO, BURIED OBJECT DETECTION
LOCKHEED ADVANCED MARINE SYSTEMS, SUNNYVALE	LOW COST MINE NEUTRALIZATION VEHICLE
MARTIN MARIETTA, BALTIMORE	LIGHTWEIGHT STRUCTURES, BONDING, AOVs, IR&D PROGRAMS
MARTIN MARIETTA, DENVER	INTELLIGENCE PROCESSING, ROBOTICS, AUTONOMOUS LAND VEHICLE
NOSC, SAN DIEGO	UNMANNED VEHICLE OVERVIEW, AOVs, ACOUSTIC LINKS, WORK FUNCTIONS
NOSC, HAWAII	DEEP VEHICLES, AUTONOMOUS VEHICLES, FIBER OPTIC CABLES, CABLE DEPLOYMENT METHODS, MARINE BIOSYSTEMS
PERRY OFFSHORE, RIVIERA BEACH	COMMERCIAL VEHICLES, MISSION SPECIFIC VEHICLES, WORK PACKAGES, MANIPULATORS
UNIVERSITY OF UTAH, SALT LAKE CITY	DEXTEROUS HAND
WESTINGHOUSE, ANNAPOLIS	PROVEN CAPABILITIES, LAUNCH/RECOVERY SYSTEMS, SUBMERSIBLE VEHICLE INTERFACE, SONARS
DEEP SUBMERGENCE LABORATORY OF WOODS HOLE OCEANOGRAPHIC INSTITUTE, FALMOUTH	DEEP SUBMERGENCE VEHICLES, IMAGING SYSTEMS, UNDERWATER SEARCH EXPERIENCE

several buses linking lower level tasks where they, in turn, could also be linked by buses to other hardware or subfunctions, etc. This hierarchial design also facilitates the implementation of Knowledge Based Systems (KBS). Choosing

the optimum buses becomes extremely important to overall system integrity and speed of response.

Next, the specific type of processor required can be chosen to match the particular levels requirements and associated algorithms. Whether one uses parallel processing, ASIC chips, DSP chips, transputers, or some hybrid combination would depend on the cost, speed and expandability required at that level. In general, a special function chip could be used at the lowest level (dedicated, application specific, stand-alone, fast, etc.) to evoke maximum performance while a state-of-the-art processor (80X86, RISC, transputer array, etc.) would handle the higher level computations which would necessarily be constantly changing with the environment and mission objectives.

Finally, the operating system must be chosen to fully utilize the hardware's performance and integrate the various levels of software. Real-time response, while supporting a multi-tasking environment, must be achieved. For future growth a symbolic language must also be supported. The ability to support limited missions has already been demonstrated, but the system level integration and cooperation needed to support a high level of Artificial Intelligence (an expert system) in an AUV is still being researched.

VI. CONCLUSIONS

A. RESULTS

Variable structure control is a highly viable control methodology for an AUV. Combining an adaptive portion of the controller with the VSC method yielded satisfactory performance considering the nonlinear nature of the problem.

Robust observers also have merit in systems with uncertainties. In our application, this technique has worked reasonably well for a range of speed and model parameter changes.

The ideal AUV architecture would most likely consist of:

- DSP or ASIC chips at the lowest level tied together with a local bus,
- special purpose processors implementing the higher levels and tied together with a smart bus (such as FUTUREBUS+), and
- a special purpose optimized real-time operating system to implement a multi-tasked hierarchical knowledge-based event-driven control system.

B. FUTURE RESEARCH

Several areas of AUV control are open to investigation and optimization. The use of DSP chips to pre-process inputs (sensor fusion) is an important area. The possibility of using Neural Networks (and associated parallel processing) to handle signal processing and control problems is a very

current and far-reaching issue. The appropriate communication links (bus type, protocol, network topology, etc.) between processors and the various control levels is a critical design choice affecting the total system performance. Eventually, a fault-tolerant system such as a Structurally Adaptive System (SAS) must be looked into to satisfy the reliability issue. A Real-Time Knowledge Based System (RKBS) should be researched as to the implementation of artificial intelligence into an AUV control system. Finally, a MIMO (Multiple-Input-Multiple-Output) VSC controller needs to be designed that takes into account all of the inputs (depth, speed, etc.), the outputs (actuators) and as accurate a model as possible in order to maximize the performance.

LIST OF REFERENCES

1. Healy, A.J., "Model Based Maneuvering Controls for Autonomous Underwater Vehicles," Mechanical Engineering Department, Naval Postgraduate School, Monterey, CA., April 1989 in review, Journal of Dynamic Systems Measurement and Control, ASME.

2. Schwartz, M.A., "Kalman Filtering for Adaptive Depth, Steering and Roll Control of An Autonomous Underwater Vehicle (AUV)," Master's Thesis, Naval Postgraduate School, Monterey, CA, March 1989.

3. Ogata, K., Modern Control Engineering, Prentice Hall, pp. 716-731, 1970.

4. Cristi, R. and Healy, A., "Adaptive Identification and Control of an Autonomous Underwater Vehicle," presented at the Sixth Annual International Symposium on Unmanned Untethered Submersible Technology, Washington, DC, June 1989.

5. Slotine, J-J. E., "Tracking Control of Nonlinear Systems Using Sliding Surfaces," PhD Dissertation, Department Aeronautics and Astrophysics, Massachusetts Institute of Technology, Cambridge, MA, May 1983.

6. Yoerger, D.R. and Slotine, J-J, E., "Robust Trajectory Control of Underwater Vehicles," IEEE Journal of Oceanic Engineering, V. OE-10, no. 4, pp. 383-388, October 1985.

7. Filippov, A.F., "Differential Equations with Discontinuous Right Hand Sides," American Math Society Translations, V. 62, pp. 199-231, 1960.

8. Kailath, T., LINEAR SYSTEMS, Prentice-Hall, pp.659-664, 1980

9. Doyle, J. and Stein G., "Robustness with Observers," IEEE Transactions on Automatic Control, v. AC-24, no. 4, pp. 607-611, August 1979.

10. Friedland, B., Control System Design, McGraw-Hill, pp. 314-321 and 455-458, 1986.

11. Leung, S.S. and Shanblatt, M.A., "Computer Architecture Design for Robotics," IEEE International Conference on Robotics and Automation, pp. 453-456, April 1988.

11. DARPA, "Unmanned Undersea Vehicle Technology Study. Volume II:Handbook," pp. 139-157, June 1986.

13. Leung, S.S. and Shanblatt, M.A., "A Conceptual Framework for Designing Robotic Computational Hardware with ASIC Technology," IEEE International Conference on Robotics and Automation, pp. 461-464, April 1988.

14. Borrill, P.L., "High-speed 32-bit buses for forward-looking computers", IEEE Spectrum, pp. 34-37, July 1989.

15. Adam, J.A., "Probing Beneath the Sea," IEEE Spectrum, pp. 56-64, April 1985.

16. Jackson, E. and Ferguson, J., "Design of ARCS - Autonomous Remotely Controlled Submersible," ROV conference, pp. 365-368, 1984.

17. Thomas, B., "Control Software in the ARCS Vehicle," Fourth International Symposium on Unmanned Untethered Submersible Technology, pp. 334-342, June 1985.

18. Jalbert, J., "EAVE III Untethered AUV Submersible," Fifteenth Annual Symposium of the Association for Unmanned Vehicle Systems, June 1988.

19. Durham, Jayson, "Progress Report for Investigating the Real-Time, or Faster, Simulation of Neural Network Models," NAVOCEANSYSCOM Memo Ser 943/81-89 of 16 Aug 89.

INITIAL DISTRIBUTION LIST

		No. Copies
1.	Defense Technical Information Center Cameron Station Alexandria, VA 22304-6145	2
2.	Library, Code 0142 Naval Postgraduate School Monterey, CA 93943-5002	2
3.	Chairman, Code 62 Department of Electrical and Computer Engineering Naval Postgraduate School Monterey, CA 93943-5004	1
4.	Department of Electrical and Computer Engineering Naval Postgraduate School Monterey, CA 93943-5004 ATTN: Professor R. Cristi, Code 62Cx	8
5.	Chairman, Code 69 Department of Mechanical Engineering Naval Postgraduate School Monterey, CA 93943-5004	2
6.	Chairman, Code 52 Department of Computer Science Naval Postgraduate School Monterey, CA 93943-5004	1
7.	Curricular Officer, Code 32 Naval Postgraduate School Monterey, CA 93943-5000	1
8.	Commander, Naval Surface Weapons Center White Oak, MD 20910 ATTN: H. Cook, Code U25	1
9.	Head, Undersea AI and Robotics Branch Naval Ocean System Center San Diego, CA 92152 ATTN: P. Heckman, Code 943	1

10. RADM Evans, SEA-92R 1
Naval Sea Systems Command
Washington, DC 20362-5101
ATTN: Ms. Judy Rumsey

11. Commander, Naval Coastal Systems Center 1
Panama City, FL 32407-5000
ATTN: Dr. G. Dobeck

12. David Taylor Naval Ship Research and 1
Development Center
Carderock Laboratory
Bethesda, MD 20084-5000
ATTN: Dr. D. Milne, Code 1563

13. Department of Mechanical Engineering 1
Naval Postgraduate School
Monterey, CA 93943-5000
ATTN: Professor F. Papoulias, Code 69Pa

14. Naval Research Laboratory 1
Marine Systems Division
Washington, DC 20375
ATTN: Dr. D. Steiger

15. Commanding Officer 2
Naval Ocean System Center
San Diego, CA 92152
ATTN: LT Michael H. Davis, Code 30

615-584

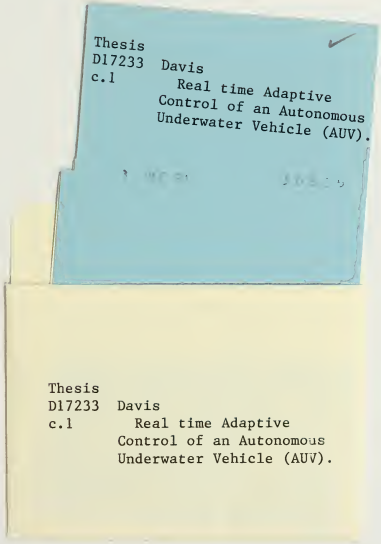
Thesis
D17233 Davis
c.1 Real time Adaptive
Control of an Autonomous
Underwater Vehicle (AUV).
Thesis
D17233 Davis
c.1 Real time Adaptive
Control of an Autonomous
Underwater Vehicle (AUV).

Real time Adaptive Control of an Autonom

3 2768 000 86405 2
DUDLEY KNOX LIBRARY